European Journal of Neuroscience, Vol. 20, pp. 2953–2962, 2004

Impaired formation of the inner retina in an AChE knockout mouse results in degeneration of all photoreceptors

Afrim H. Bytyqi,[1] Oksana Lockridge,[2] Ellen Duysen,[2] Yuxia Wang,[2] Uwe Wolfrum[3] and Paul G. Layer[1]
[1]Darmstadt University of Technology, Developmental Biology & Neurogenetics, D-64287 Darmstadt, Germany
[2]Eppley Institute, Department Biochemistry, University of Nebraska, Omaha NE 68198–6805, USA
[3]Johannes-Gutenberg University Mainz, Institute for Zoology, D-55099 Mainz, Germany

Keywords: acetylcholine, cholinergic system, inner plexiform layer, lamination, retinal development, photoreceptors

Abstract

Blinding diseases can be assigned predominantly to genetic defects of the photoreceptor/pigmented epithelium complex. As an alternative, we show here for an acetylcholinesterase (AChE) knockout mouse that photoreceptor degeneration follows an impaired development of the inner retina. During the first 15 postnatal days of the AChE$^{-/-}$ retina, three major calretinin sublaminae of the inner plexiform layer (IPL) are disturbed. Thereby, processes of amacrine and ganglion cells diffusely criss-cross throughout the IPL. In contrast, parvalbumin cells present a nonlaminar IPL pattern in the wild-type, but in the AChE$^{-/-}$ mouse their processes become structured within two 'novel' sublaminae. During this early period, photoreceptors become arranged regularly and at a normal rate in the AChE$^{-/-}$ retina. However, during the following 75 days, first their outer segments, and then the entire photoreceptor layer completely degenerate by apoptosis. Eventually, cells of the inner retina also undergo apoptosis. As butyrylcholinesterase (BChE) is present at a normal level in the AChE$^{-/-}$ mouse, the observed effects must be solely due to the missing AChE. These are the first *in vivo* findings to show a decisive role for AChE in the formation of the inner retinal network, which, when absent, ultimately results in photoreceptor degeneration.

Introduction

Blinding diseases affect a very large number of people, so that every six seconds one person becomes blind in Europe. Retinitis pigmentosa (RP), age-related macular degeneration (AMD), and numerous variations of similar blinding diseases are manifested along with degeneration of photoreceptors. Appropriate animal models are extremely important to study molecular defects causing blinding diseases, noticeably the rd mouse, the rds mouse and the RCS rat (Farber *et al*., 1991; LaVail, 2001; see also Discussion). Most available data led to the assumption that degeneration of photoreceptors, and therefore most blinding diseases, originate from genetic defects of the photoreceptor and pigmented epithelium complex (Molday, 1998; see also Discussion).

The formation of a retina is an intricate process, governed by cell-autonomous, as well as cell-interactive mechanisms. While photoreceptors together with ganglion cells are born early, photoreceptors differentiate relatively late. In general, the differentiation and wiring of the inner retina precedes that of the outer retina. It seems plausible that early developmental wiring defects could, through retina-internal cell interactions, eventually lead to degeneration of photoreceptors. The present studies on the development (P1–P20) and degeneration of retinae (until P266) from an AChE$^{-/-}$ knockout mouse support such mechanisms.

This raises the question as to what roles the cholinergic system plays in retinal development. In general, the significance of neurotransmitter systems for proper neural development has been studied extensively (Kater & Lipton, 1995; Lauder & Schambra, 1999; Buznikov *et al*., 2001). ACh is not a predominant neurotransmitter of the retina, but nevertheless the cholinergic system plays a pivotal role in the physiology and the development of a normal retina. In all vertebrate retinae, two rows of putative cholinergic amacrine cells are found on either side of the IPL. These starburst amacrine cells with their delicate morphology are involved in generation of waves of spontaneous nicotinic activity and activity-dependent wiring of the retina (Wong *et al*., 2000; Sernagor *et al*., 2001; Zhou, 1998, 2001). AChE, as one component of the cholinergic system, is expressed very early in the retina after the last cell division and precedes neuritic outgrowth (Layer, 1990). Along with the emergence of an IPL, the enzyme is expressed in two major subbands long before its counterpart ChAT appears and before synaptogenesis in the IPL (Layer *et al*., 1997), suggesting that AChE has a developmental role in the inner retina. There is ample evidence showing neuritogenic role(s) of AChE, which, depending on the system, can be assigned to either the catalytic activity and/or noncatalytic parts of this protein. As most of these data have come from *in vitro* studies, an AChE$^{-/-}$ mouse was established. In the first part of this study, we have analysed the postnatal retinal development with particular emphasis on the inner retina including sublamina formation in the IPL. Using antibodies to three calcium binding proteins as markers, we have documented that the early wiring of the IPL is dramatically changed. These changes begin to be detected while the overall layering of the AChE$^{-/-}$ retina appears nearly normal. Subsequently, all photoreceptors in the AChE$^{-/-}$ retina eventually degenerate over an extended postnatal period. These findings assign a prominent and indispensable role(s) to AChE in development of the inner retina, as in maintenance of all photoreceptors.

Correspondence: Professor Paul Layer, as above.
E-mail: layer@tu-darmstadt.de

Received 5 April 2004, revised 10 September 2004, accepted 20 September 2004

doi:10.1111/j.1460-9568.2004.03753.x

Materials and methods

Animals and eyes

The Institutional Animal Care and Use Committee of the University of Nebraska Medical Center approved all procedures involving mice. Animal care was provided in accordance with the principles and procedures outlined in the National Institutes of Health Guide for the Care and Use of Laboratory Animals. AChE$^{-/-}$ mice in strain 129Sv were made by gene-targeting. These mice have no AChE protein and no AChE activity as the entire ACHE gene was deleted (Xie *et al*., 2000). Animals were killed by decapitation. Eyes from 75 homozygous AChE$^{-/-}$ and 65 wild-type (WT) mice were isolated, and dissected free of connective tissue in the laboratory of Oksana Lockridge (Omaha). The eyes were immediately fixed in 4% paraformaldehyde dissolved in phosphate buffered saline (PBS) for 2 h at room temperature. After fixation, the eyes were washed three times in phosphate buffered saline for 15 min and then transferred overnight into a solution of 25% sucrose/PBS. Fixed eyes were shipped on dry ice by express mail. A full series of fixed eyes from P1 through P19, and adult eyes for P36 to P266 were at our disposal. The eyes were kept at 4 °C until their sectioning at 10–16 μm on a cryostat (Microm, Walldorf, Germany). AChE$^{-/-}$ mice open their eyes on P13–14, one or two days later than wild-type mice; these mice have pinpoint pupils throughout life. Animals were reared in a 12-h light : 12-h dark cycle.

Immunostainings

Cryosections were dried at 37 °C and then washed three times for 5 min each with PBS. Retinal sections were blocked for 40 min in a solution of 3% bovine serum albumin (BSA), 0.5% Triton X-100 in PBS. The primary antibodies were diluted in PBS containing 1% Triton X-100 and applied for 2 h at room temperature. Three washes with PBS (10 min each) were followed by incubation with the secondary antibody for 1 h at room temperature. Finally, the sections were stained with DAPI (4′, 6-diamidine-2-phenylindol-dihydrochloride; Boehringer, Mannheim; 0.1 μg/mL), washed in distilled water and mounted in Kaiser's glycerol gelatine (Merck, Darmstadt, Germany). For controls, the primary antibody was omitted.

Primary antibodies

Photoreceptor cells were labelled with a mouse anti-rho4D2 diluted 1 : 2000 (Molday, 1988), generous gift from Dr D. Hicks, Strasbourg, France). Amacrine and displaced amacrine cells were detected with a rabbit-anti Calretinin polyclonal antibody, diluted 1 : 2000 (Swant, Bellinzona, Switzerland; Pasteels *et al*., 1990) and a calbindin polyclonal antibody, dilution 1 : 1000 (Swant, Bellinzona, Switzerland). A monoclonal antibody against glutamine synthetase is specific for Müller cells, diluted 1 : 2000 (DB, Bioscience, Heidelberg, Germany; Prada *et al*., 1988); a polyclonal antibody against parvalbumin is specific for AII amacrine cells and α-like ganglion cells, diluted 1 : 1000 (Wässle *et al*., 1993; Casini *et al*., 1995). For specific rod photoreceptor staining, the mouse anti-rho4D2 was used at a 1 : 2000 dilution (Molday, 1988; generous gift of Dr D. Hicks, Strasbourg, France). CY^3-conjugated goat-anti-rabbit and rabbit-anti-mouse IgG were used as secondary antibodies (IgG; 1 : 100 dilution, Dianova, Hamburg, Germany).

Electron microscopy

Eyes were sectioned, washed three times with PBS and fixed in 2% glutaraldehyde in 0.1 M cacodylate buffer, pH 7.4 for 30 min. The tissue was then postfixed in 1% OsO_4 in cacodylate buffer for 30 min at 4 °C, dehydrated in a graded series of ethanol (25–100%), followed by propylene oxide, and embedded in Epon 812 (Serva, Heidelberg, Germany). Ultrathin sections were cut, stained with uranyl citrate, and investigated with a ZEISS EM10 electron microscope.

In situ *cell death detection by TdT-mediated dUTP nick end labelling (TUNEL assay)*

The TUNEL reaction preferentially labels DNA strand breaks generated during apoptosis. Paraformaldehyde-fixed cryosections of eyes were incubated in permeabilization solution (0.1% Triton X-100, 0.1% sodium citrate) for 2 min on ice (4 °C). The slides were rinsed twice with PBS. Fifty-microlitres of TUNEL reaction mixture (50 μL terminal deoxynucleotidyl transferase from calf thymus; EC 2.7.7.31) were diluted in 450 μL label solution (nucleotide mixture, according to the manual of Boehringer Mannheim, Germany). The slides were incubated with this mixture in a humidified chamber for 60 min at 37 °C in the dark, then rinsed three times with PBS and embedded with Mowiol. Sections were then analysed under a fluorescence microscope, and the number of dead cells per 500 total cells was counted.

BChE activity in isolated retinae

The assay was adapted from the method of Johnson & Russell (1975). Three male AChE$^{-/-}$ (P118, P169, P182) and three male wild-type (P61, P102, P121) mice strain 129Sv were used for this experiment. Animals were decapitated and the retina dissected from the eyes. The retinas were stored at −70 °C. A whole retina was incubated in 100 μL total volume containing 0.05 M potassium phosphate pH 7.0, 50 μM 3H-butyrylcholine, and 20 μM BW284C51 (1,5 bi(4-allyldimethyl ammonium phenyl)-pentan-3-one (Sigma, #A9013). The BW was added to inhibit AChE in the wild-type samples, though all samples were treated with BW. The 3H-butyrylcholine was custom synthesized by Perkin-Elmer (Boston, MA) and was diluted to a specific activity of 0.37 Ci/mmole. The 100 μL reaction mixture was incubated in a scintillation vial for 70 min at 25 °C. The reaction was stopped by the addition of 200 μL stop mixture (1 M chloroacetic acid, 0.5 M NaOH, 2 M NaCl). The stop mixture neutralized the butyrate and thus allowed separation of the neutral 3H-butyrate from the positively charged choline product after addition of 4 mL of a toluene scintillation cocktail. The scintillation cocktail was made up of 8 mL rpi scintillator (#111023, Research Products International Corp., Mount Prospect, IL), 33.3 mL isoamyl alcohol, and 159 mL toluene. Vials were vigorously shaken and then the phases were allowed to separate for 1 h before the vials were counted. Human serum was used as a standard for the assay. The BChE activity of the human serum was measured in the spectrophotometer in the Ellman assay where the butyrylthiocholine concentration was 1 mM, and the buffer was 0.1 M potassium phosphate pH 7.0. Human serum with an activity of 2.74 μmoles butyrylthiocholine per min per ml, was diluted 100-fold. One to nine microlitres of the 1 : 100 diluted human serum were assayed with radiolabelled 3H-butyrylcholine under conditions identical to those described above.

Microscopy and photography

The sections were photographed with a photomicroscope (Axiophot; Zeiss, Jena Germany) using 10×, 20×, and 40× objectives and the appropriate fluorescence filters. Micrographs were taken using a

digital camera (INTAS 3-CCD; Intas, Göttingen, Germany), processed with Adobe Photoshop and printed using an Epson Stylus Color 740 printer.

Results

Severe developmental distortions of inner retinal network

The development of AChE$^{-/-}$ retinae is abnormal. The most significant differences between developmental patterns of the AChE$^{-/-}$ mouse retina and the normal retina were revealed by applying immunostaining for the calcium-binding proteins, calbindin (CB), calretinin (CR), and parvalbumin (PV). Calbindin labelled three major cell types (Fig. 1). Cells of the ganglion cell layer (GCL) were first detectable before P5; the patterns being similar in both mice. Only slightly later, CB was also found in a row of amacrine (Fig. 1A and E), and, before P9, a row of horizontal cells of the inner nuclear layer (INL). Their processes formed three distinct sublaminae of the IPL; they also fasciculated more diffusely in the outer plexiform layer (OPL) (Fig. 1B). In the AChE$^{-/-}$ mouse retina, all three cell systems became detectable later, but the number and individual sizes of cells were diminished (Fig. 1F). Sublaminae formation in the IPL of the AChE$^{-/-}$ mouse retina was much less organized and was delayed (cf. Fig. 1B–D, and F–H). The third (middle) sublamina developed only after P19 (Fig. 2G and H). In the adult AChE$^{-/-}$ retina, the pattern became almost normal, presenting three IPL sublaminae (Fig. 1H), but the ratio and density of labelled cells was still less than normal. Noticeably, here the OPL staining indicated a tighter fasciculation than in the wild-type. More striking differences between wild-type and AChE$^{-/-}$ mouse retina were revealed by calretinin staining (Fig. 2). In the wild-type retina (Fig. 2A–E), ganglion cells and then of a subpopulation of amacrine cells were strongly stained. Their processes into the IPL formed three distinctly labelled sublaminae; a fourth one next to the border INL/IPL was weakly labelled. Processes of ganglion cells into the optic fibre layer (OFL) were strongly stained (Fig. 2B–D). This staining pattern developed from P1 onwards, both in the wild-type and in the AChE$^{-/-}$ mouse retina (Fig. 2A and F). However, in the latter, the staining pattern at P5 was much weaker, in particular on the amacrine cell side (Fig. 2B and G). During the following period up to P9 (Fig. 2C and H), their processes did not organize into three sublaminae, but criss-crossed in a diffuse manner throughout the IPL (see also Fig. 3B). Sizes of both ganglion and amacrine cells were highly variable (Fig. 2F and I). Only after a long delay, did the diffuse processes eventually organize into three sublaminae (Fig. 2J); the final pattern was then similar to the wild-type retina, but the number of stained cells was still drastically reduced.

Parvalbumin (PV) staining presented entirely novel patterns for the AChE$^{-/-}$ mouse retina (Fig. 3C and D). While both calbindin and calretinin staining could have been conceived of as reductions of

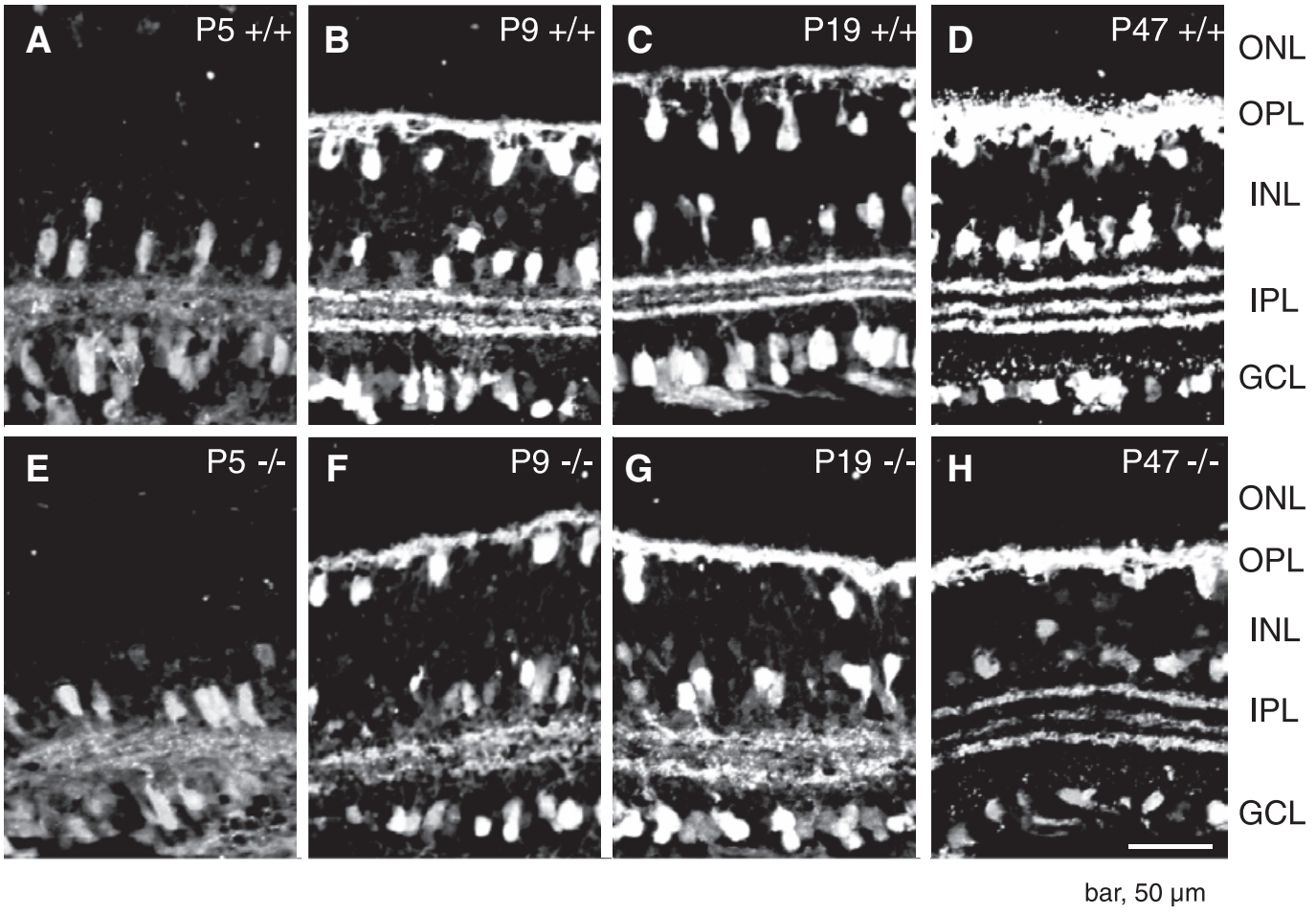

FIG. 1. Decrease of calbindin (CB)-positive cells and delay of their IPL stratification in the AChE$^{-/-}$ mouse retina (lower; wild-type on upper), as revealed by immunostaining of P5 (A and E), P9 (B and F), P19 (C and G) and P74 (D and H). Note that all CB-positive cell populations, horizontal, amacrine and ganglion cells are affected; final adult IPL subband pattern is similar in both animals, but labelled cells are still fewer in AChE$^{-/-}$ retina. Scale bar, 50 µm.

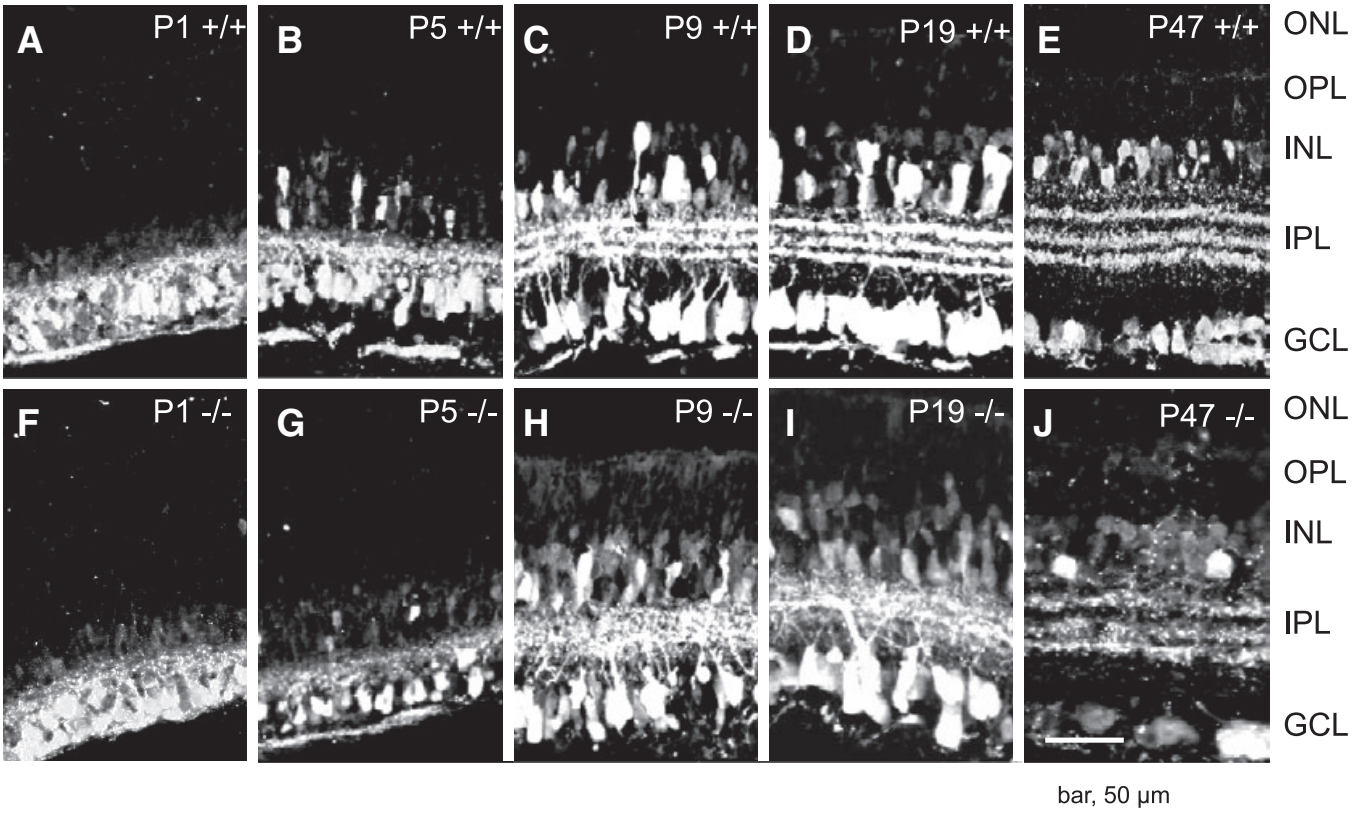

FIG. 2. Severe developmental distortions of IPL stratification in the AChE$^{-/-}$ mouse retina (lower; wild-type on upper), as revealed by calretinin immunostaining. Staining at P1 mainly on future GCL is similar in both animals (A and F). Note delay at P5 (G, cf. B), highly disorganized neuritic growth at P9 (H, cf. C; see also Fig. 3B) and P19 (I, cf. D); while final adult patterns at P47 (J, cf. E) are similar, although CR^{+} cells are still fewer in AChE$^{-/-}$ retina. Scale bar, 50 µm.

structural organization, stunningly, the PV-positive cell system showed an increased degree of tissue organization (Fig. 3D). As described in the literature, PV-labelled ganglion cells in the wild-type retina sent their processes into the IPL in a diffuse manner (Fig. 3C); in addition, a minor staining was detected in the OPL. In contrast, in the AChE$^{-/-}$ mouse retina, starting on P5, processes of ganglion cells into the IPL tended to arrange into parallel multiple subbands (not shown). At adult stages (from 31 to P47) two clearly defined IPL subbands were established (Fig. 3D). At very late stages in the AChE$^{-/-}$ mouse retina the parvalbumin staining disappeared altogether (not shown).

The differential course of retinal development was also reflected by a changed morphology of Müller cells (MC), as detected by immunostaining for glutamine synthetase (GS, see Fig. 3E and F for adults). Already at P9, an irregular arrangement of cell processes was evident; by P11 the staining of MC cell bodies was much weaker. By P19, the outer nuclear layer (ONL) was thinner; the photoreceptor somata were less well organized compared with the wild-type retina (not shown).

Degeneration of the ONL

From approximately 1.5 months onwards, the AChE$^{-/-}$ retina began to show signs of laminar degeneration. DAPI-stained sections showed that by P47, the ONL had begun to thin out (Fig. 4C); by P88 the thickness of the ONL had narrowed from approximately 15 cell bodies-wide to 2–3 cell-bodies wide (Fig. 4D). Depending on the individual animal and the particular retinal location, a one cell-wide layer sometimes remained in the ONL until P167 (Fig. 4E). Quantitative measures showed that generally after approximately three months the ONL together with the OPL had completely disappeared (not shown).

Outer segments are the first to degenerate

To follow the fate of the outer segments in detail, we used the rod-specific rho4D2 antibody (Fig. 5). The spatial arrangement of AChE$^{-/-}$ outer segments appeared nearly normal up to one month (P31; Fig. 5B), by P47 their length was reduced (Fig. 5C). Over an extended period of approximately 40 days, rhodopsin staining diminished (Fig. 5D), to eventually vanish completely. This was supported by EM studies revealing a pronounced malformation of outer segments (Fig. 6). The regular arrangement of membrane stacks in outer segments of the wild-type retina was completely disorganized in AChE$^{-/-}$; all outer segments were fragmented in the AChE$^{-/-}$ retina. As documented in Figs 4 and 5, deterioration of outer segments preceded that of ONL and OPL, and therefore was the first sign of retinal degeneration in the AChE$^{-/-}$ retina.

Degeneration is due to programmed cell death

To follow the death of cells, the TUNEL assay was applied to sections of different stages from wild-type and AChE$^{-/-}$ retinae (Fig. 7). From P19 onwards, an increasing number of apoptotic cells was detected in the ONL, while no significant apoptotic cells were found in the wild-type retina (not shown). Determination of the ratio of TUNEL-positive cells showed (Fig. 8) that maximal cell death was reached around P60–70; by P88 almost all cells were gone from the ONL (cf. Fig. 4).

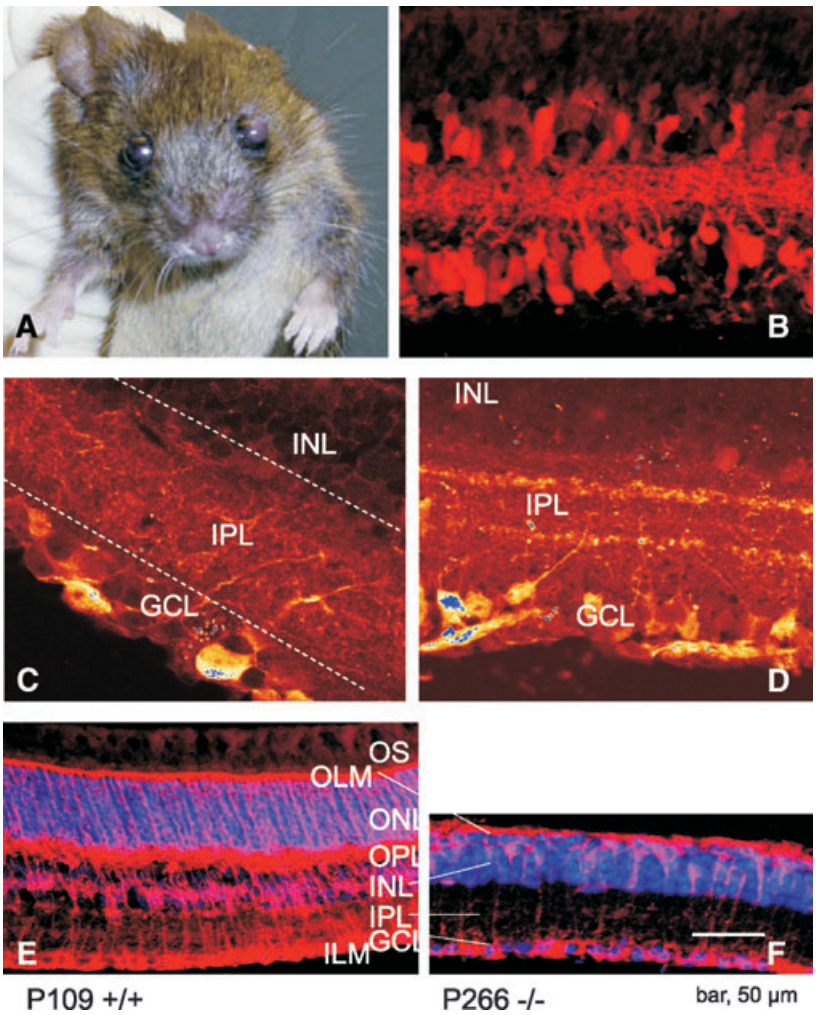

FIG. 3. (A) AChE$^{-/-}$ mouse with bulging eyes. (B) Details of calretinin staining in IPL of P9 AChE$^{-/-}$ retina. Note irregular courses of neurites from ganglion (lower row) and amacrine cells (upper). (C and D) Parvalbumin (PA) staining is diffuse in adult retina of WT mouse (C; broken lines indicate space of IPL), but presents laminar order in retina of AChE$^{-/-}$ mouse (D), as shown for P47. Note two 'novel' sublaminae in IPL of AChE$^{-/-}$ retina (D). (E and F) Müller cell morphology reveals drastic alterations in adult AChE$^{-/-}$ retina. Sections of a wild-type P109 (E) and a P266 AChE$^{-/-}$ retina (F) were stained for glutamine synthetase and DAPI, as described in Materials and methods. Note reduced width and almost absent staining of IPL in the AChE$^{-/-}$ retina. Scale bar, 50 µm.

Only later, after the period of cell death had faded out, were more and more apoptotic cells detected in the INL (Fig. 7, lower); at late stages even the few remaining cells in the GCL became apoptotic (Fig. 7, lower, arrow). Thus, cell death occurred in a graded manner from the retinal outside to more inner aspects.

Müller glia cells deteriorate

Death of cells in the ONL and then in the INL is accompanied by drastic changes of the typical Müller glial scaffold. This scaffold as shown for a P109 wild-type retina (Fig. 3E) by glutamine synthetase (GS) staining was absent in the AChE$^{-/-}$ retina (Fig. 3F, showing P266). Most noticeably, the organization of the inner limiting membrane (ILM) appeared weaker and less filigrane; cell bodies of Müller cells were shifted to more outer locations and many radial fibers appeared dislodged. At late stages (P266), labelling of the IPL (branchlets of Müller cells) and of the OPL (rootlets of Müller cells) was almost completely missing; at the ILM, individual Müller cell endfeet stood out, and stained radial fibers had become few; the outer limiting membrane (OLM) began disassembling.

BChE activity in AChE$^{-/-}$ mouse retina is not altered

Finally, we tested whether BChE is altered in the AChE$^{-/-}$ retina, and thus could be (partially) responsible for the observed changes in the AChE$^{-/-}$ retina. For this purpose a radiometric assay was developed for measuring BChE activity in isolated retinae (Fig. 9). AChE$^{-/-}$ and AChE$^{+/+}$ retinas had similar BChE activities of 6382 ± 743 and 5947 ± 428 cpm/70 min × retina, respectively ($n = 6$ for each group). The BChE activity in a single retina was equivalent to the BChE activity in 0.04 µL of human serum.

Discussion

Eyes of AChE$^{-/-}$ mice are deformed

This represents the first *in vivo* study in a mammal demonstrating a significant developmental role for AChE. Surprisingly, AChE$^{-/-}$ mouse survive to adulthood in the absence of any AChE activity or AChE protein, although growth and behavioural problems were apparent (Li *et al*., 2000; Xie *et al*., 2000; Duysen *et al*., 2002). It is assumed that the related enzyme BChE, or possibly less specific

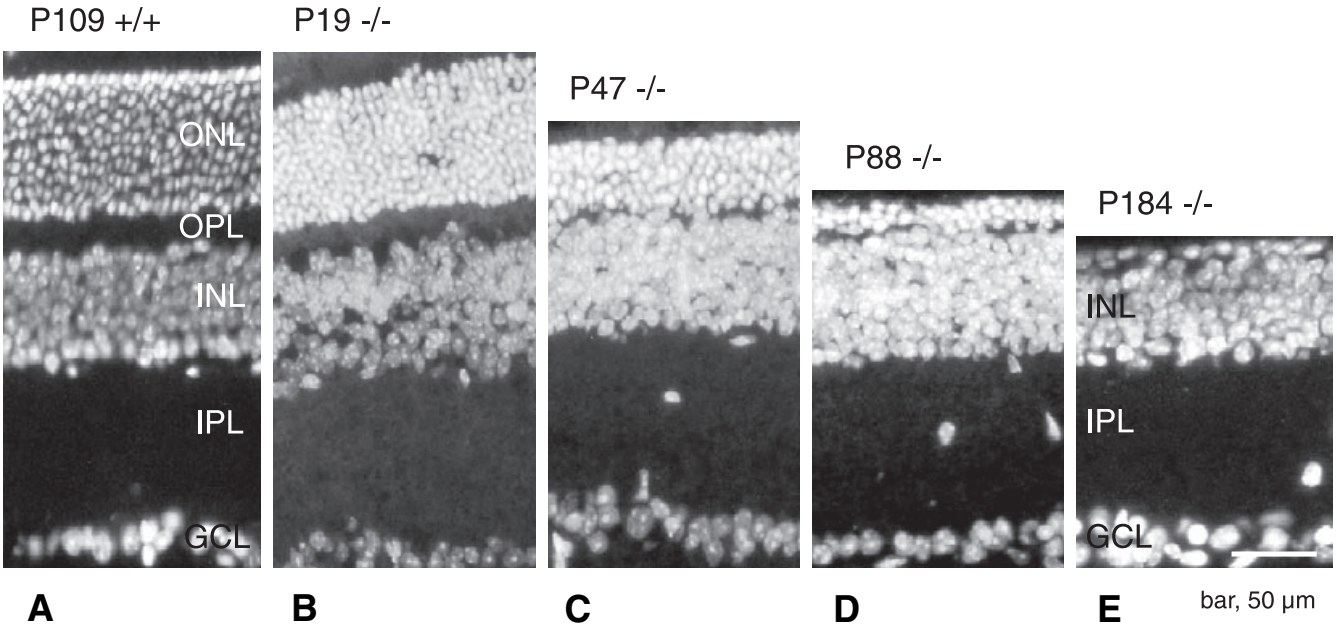

FIG. 4. Reduction of width of ONL in AChE$^{-/-}$ mouse retina, as shown by DAPI-stained cryosections from P19 to P164. For comparison, a wild-type P109 retina is shown on left.

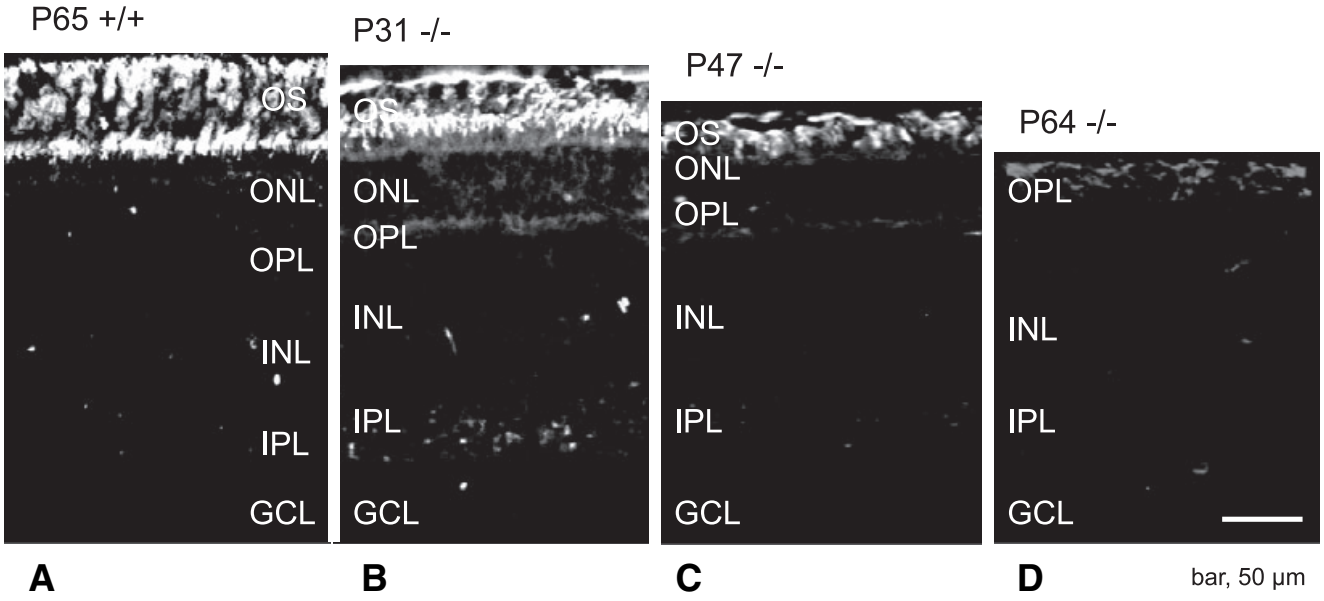

FIG. 5. Degeneration of outer segments, as shown by rho4D2 antibody staining on transverse cryosections of wild-type and AChE$^{-/-}$ mouse retina. Section in left shows a mature wild-type mouse retina at P65. The gradual disappearance of photoreceptors in the AChE$^{-/-}$ mouse starts around P30. At this stage the outer segments are well differentiated, but reduced in size. At P64 the AChE$^{-/-}$ mouse presents a very weak immuno-reactivity to rho4D2 showing that the outer segments (OS) have degenerated. Scale bar, 50 µm.

esterases, compensate for the absence of AChE. Clearly, these mice are developmentally delayed; their eyes open on P13–14, one or two days later than in wild-type mice. AChE$^{-/-}$ mice have pinpoint pupils throughout life. On visual inspection the eyes of young animals look normal, but in many animals older than P100, the eyes bulge out (Fig. 3A). In some animals the bulging eyes become covered with a vascular bed. Some older AChE$^{-/-}$ animals have one bulging eye and one sunken eye. The sunken eyes are surrounded by a hairless rim, the hair having been pulled off by the mucus exudate that flows from the sunken eyes. All AChE$^{-/-}$ mice older than one year have eyes that look abnormal. Although the cholinergic regions of their brains appeared normal (Mesulam *et al.*, 2002), these obvious eye defects prompted us to investigate the development and fate of their retinae. We found that the retina of the AChE-deficient mouse does not develop normally and eventually deteriorates. How could loss of photoreceptors in adult life be linked with developmental defects in this mouse?

Photoreceptor degeneration originating from the inner retina?

For the analysis of blinding diseases, three rodent mutants showing degenerating photoreceptors have played a pivotal role. In the rd mouse, cGMP levels play a major role (Lolley *et al.*, 1977; Farber

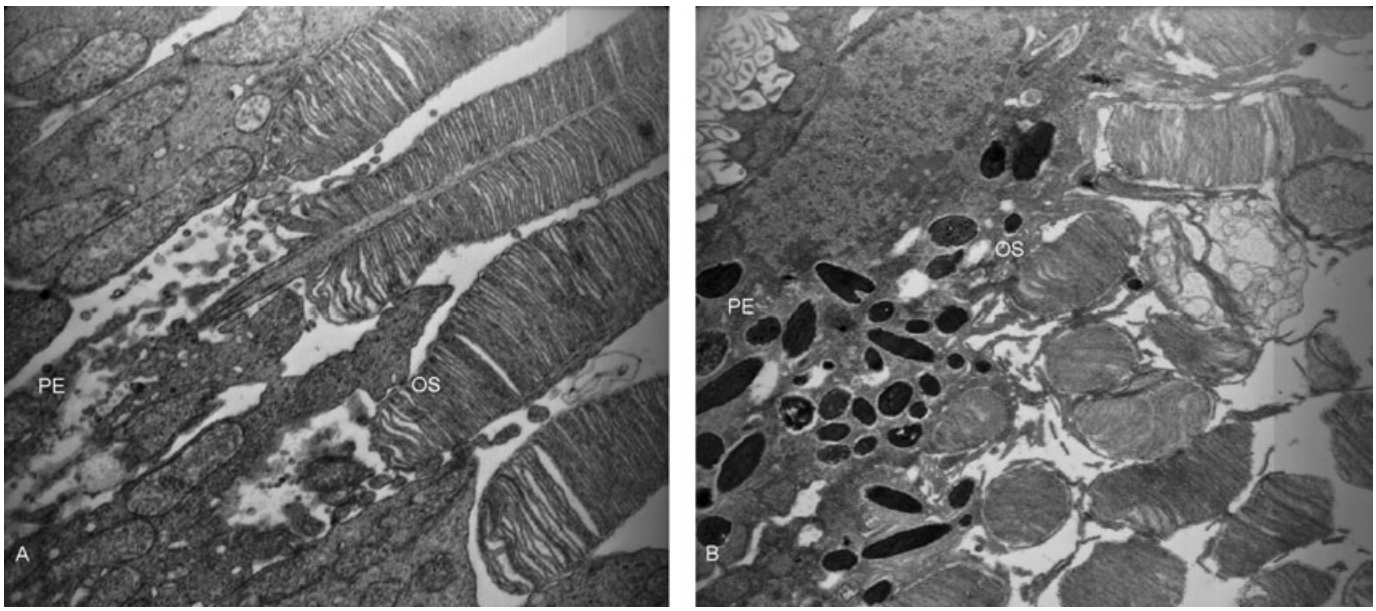

FIG. 6. Electron micrograph showing degeneration of outer segments in AChE$^{-/-}$ retina. Note regular membrane stacks in outer segments of WT (left), while they are short and fragmented in knockout retina (right). PE, pigmented epithelium.

et al., 1991), while in the rds mouse, peripherin in outer segments is mutated (Travis *et al*., 1989; Connell *et al*., 1991). In the retinal dystrophic rat, also known as the RCS rat model for retinitis pigmentosa (Bourne *et al*., 1938; Dowling & Sidman, 1962; LaVail, 1981, 2001), pigmented epithelial cells fail to phagocytize shed rod outer segments. The ONL almost completely disappears within 55 days. Transplantation of pigmented epithelial cells into the subretinal space of RCS rats can rescue photoreceptors (Li & Turner, 1988; see LaVail, 2001). Together, these findings led to the assumption that degeneration of photoreceptors (and therefore most blinding diseases) originates from defects of the photoreceptor/pigmented epithelial complex (Molday, 1998; Aguirre *et al*., 2002).

In the AChE$^{-/-}$ retina all photoreceptors degenerated after three months, a somewhat extended period when compared with the animal models described above. At present it remains open whether photoreceptors before their degeneration become physiologically active. However, behavioural observations indicate that the animals never can see. This issue is presently further analysed by measuring electroretinograms in young and older animals. As photoreceptor degeneration is a late event, we wondered whether deterioration of the outer retina could be a consequence of earlier wiring defects primarily afflicting the inner retina. Such a dependence of photoreceptors from 'downstream signals' was shown in a transgenic swine carrying a rod-specific mutation. In this case, rod afferent activity affected the postnatal maturation of cone retinal circuitry (Banin *et al*., 1999).

Wiring of inner AChE$^{-/-}$ retina: not only destruction, but a new order

During postnatal development, there were no gross alterations of the AChE$^{-/-}$ retina. Our estimates indicated that cell numbers in the GCL and in the INL of the AChE$^{-/-}$ retina were close to normal, while the number of photoreceptor cell rows always remained somewhat reduced. Moreover, cells in the AChE$^{-/-}$ retina appeared spatially less organized. In particular in the ONL, a strict columnar separation of cells was missing.

In mice, stratification of the retina commences shortly after birth. Early events in retinogenesis are the formation of a GCL and then INL, followed by differentiation of ganglion and amacrine cells. Subbands in the IPL of all vertebrates are formed by (fasciculating) processes from specific subpopulations of ganglion, amacrine and bipolar cells. For their inspection, parvalbumin, calbindin and calretinin were chosen as markers among the many calcium-binding proteins in the nervous system, because they are particularly striking in their abundance and in specificity of their distribution (Baimbridge *et al*., 1992). For instance, CR, CB and PV are useful to distinguish between subpopulations of amacrine, bipolar and horizontal cells (Jeon *et al*., 2001; Dmitrieva *et al*., 2003; Kablar, 2003), e.g. calretinin stains AII amacrine cells in primates (Scher *et al*., 2003). Development of all three CaBP systems was specifically affected in the AChE$^{-/-}$ retina. Particularly, the results for the parvalbumin (PV) system were striking, as a transient establishment of two novel subbands in the AChE$^{-/-}$ retina was documented. Normally, PV-positive ganglion cells send prominent processes at an oblique angle into the IPL, which then diverge into a diffuse meshwork distributed over its entire width. This is evidence that in the absence of AChE protein and AChE activity, not only a reduction of network order can occur (which could be interpreted as indicating a mere destruction of the tissue), but a new spatial order is established.

Degeneration of outer and then inner retina involves Müller cells

Analysis of the temporal changes of cell layers on the basis of DAPI stained sections showed that outer segments and the ONL are the first to degenerate, followed by a diminution of the INL. TUNEL stainings indicated, that after complete degeneration of the ONL, apoptotic cells appear consecutively from outside to inside. The width of the IPL remains stable in the AChE$^{-/-}$ retina, which is striking, as its Müller glia is deteriorating, including a dislocation of cell bodies and radial fibers. The total mass of neuropil material in the IPL supposedly does not change in the AChE$^{-/-}$ retina, but the laminar organization might be impaired (e.g. by defasciculation). In fact, in some models of induced photoreceptor degeneration, a marked Müller cell response has been noted (Fisher *et al*., 2001), including increased expression of vimentin (Willbold & Layer, 1998). A similar response may be effective during earlier periods of the AChE$^{-/-}$ retina, while later the glial scaffold clearly is regressing.

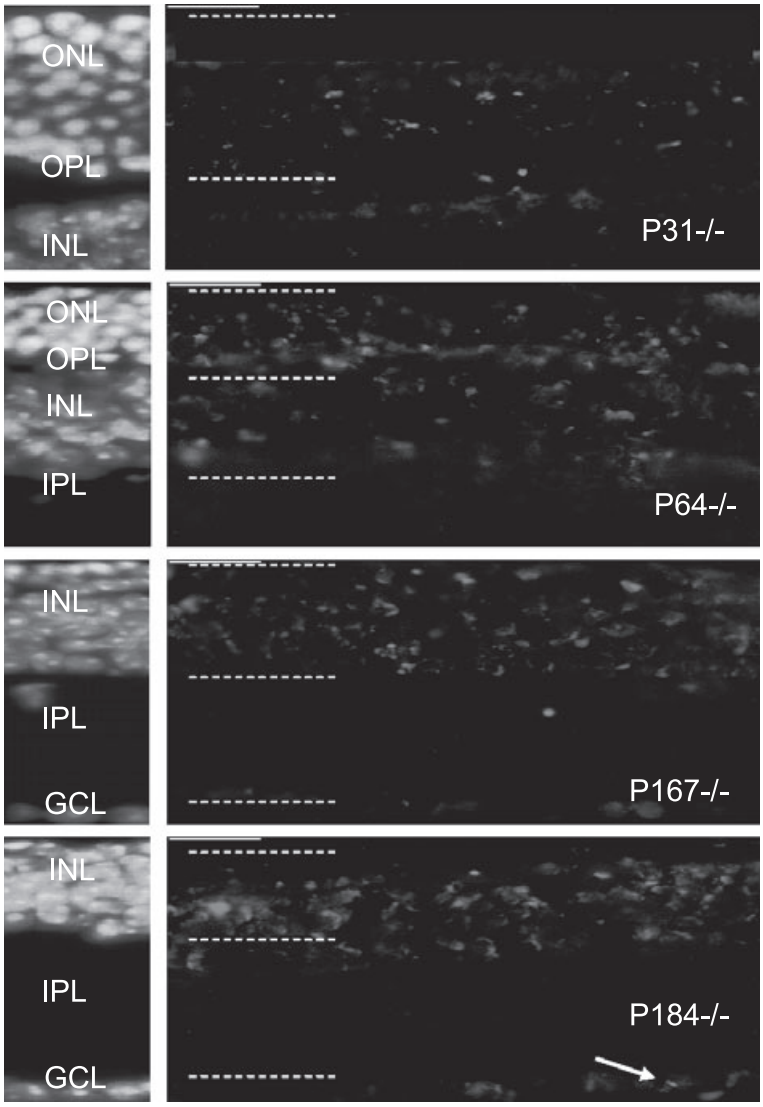

FIG. 7. Apoptotic cells in AChE$^{-/-}$ retinae, as detected by TUNEL assay (right; on left DAPI stained sections of the same frames). Note that apoptotic cells at younger stages are detected only in ONL, but with time appear also in INL and eventually even in GCL (arrow). Broken lines outline relevant nuclear layers. Scale bar, 50 μm.

Cholinergic mechanisms in retinogenesis and maintenance?

This study shows that a missing AChE in the mouse strongly interferes with normal retinogenesis and its maintenance. How could AChE work in the retina? Starburst amacrine cells constitute the major cholinergic cell population in the vertebrate retina. With their long horizontal processes organized within two sublaminae of the IPL, they are presynaptic to bipolar, ganglion and other amacrine cells. Moreover, a large variety of cells including horizontal cells are cholinoceptive, as shown by the distribution of muscarinic and nicotinic ACh receptor subtypes (Yamada *et al.*, 2003). Also, synapses between subpopulations of photoreceptors and horizontal cells are cholinergic (Cuenca *et al.*, 2000). This indicates that ACh influences many cells in all retinal layers. In the mature mouse retina, most cells seem to express AChE (Broide *et al.*, 1999). However, during development of avians, a strong AChE expression in postmitotic ganglion and amacrine cells demarcates the inner retinal half, representing a first constituent of the cholinergic system (Layer, 1990). Shortly thereafter, two AChE-positive IPL subbands (Reiss *et al.*, 1997) are part of the cholinergic starburst amacrine system, preceding synaptogenesis in the IPL and announcing a structural segregation into physiological ON and OFF channels (Layer *et al.*, 1997). This same cholinergic system later initiates spontaneous cholinergic activity, which possibly could shape

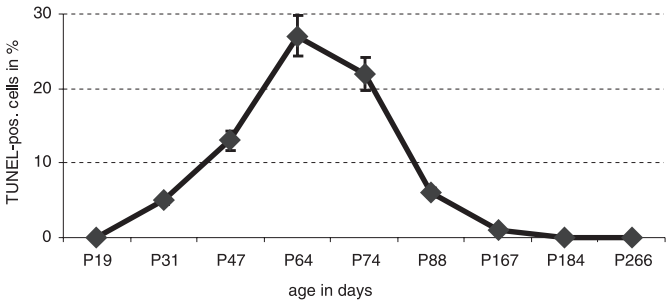

FIG. 8. Time-course of TUNEL^{+} apoptotic cells in AChE$^{-/-}$ retina. At P31 the first apoptotic nuclei were detected, followed by a rapid increase until apoptosis reached a maximum of 27% by P64; by P88 only very few TUNEL^{+} cells remained detectable. The decrease in the number of apoptotic photoreceptors correlated with the disappearance of the photoreceptor layer (ONL). The process was complete by postnatal day 167.

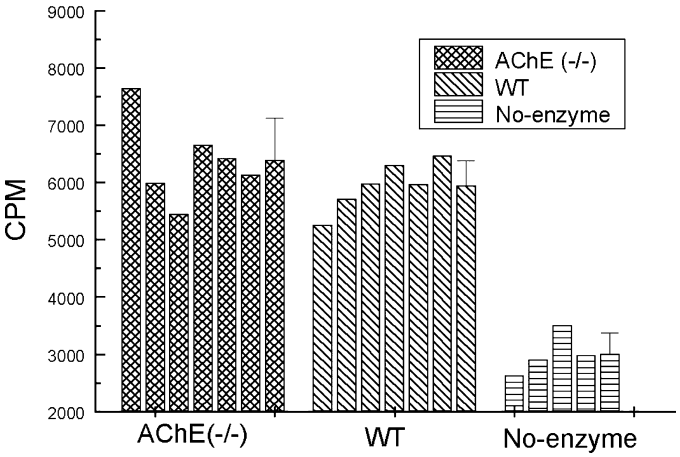

FIG. 9. Radiometric determinations of BChE activities show no significant differences between AChE$^{-/-}$ and WT mouse retinae. Six retinae from three animals were determined for each group; the last column in each group is the mean value for each set; 'no-enzyme' shows control measurements in absence of retina.

activity-dependent wiring of the retina (Wong *et al*., 2000; Zhou, 2001).

Is there a link between the early established starburst system and photoreceptors? Indeed, prior to the differentiation of outer segments in the ferret retina, photoreceptors transiently target to a distinct IPL sublamina coincident with cholinergic amacrine cell processes (Johnson *et al*., 2001). After excitotoxic elimination of cholinergic amacrine cells, rod terminals were found throughout the depth of the IPL, as well as extending into the GCL. Thus, targeting of photoreceptor terminals to discrete strata within the IPL depends upon cholinergic amacrine cell processes. It may very well be that in the AChE$^{-/-}$ retina a defect in this early connection between IPL and photoreceptors causes a delayed degeneration of outer segments and then further of the ONL and INL. It will be interesting to find out whether in the AChE$^{-/-}$ retina, only AChE activity is missing, or whether the cholinergic starburst cells are missing altogether.

How AChE affects neural development is still much debated (the literature is too extensive, for reviews see Layer & Willbold, 1995; Grisaru *et al*., 1999; Radic & Taylor, 2001; Scholl & Scheiffele, 2003). Neuromuscular development was disturbed in a mutant AChE$^{-/-}$ zebrafish (Behra *et al*., 2002), and cholinesterase inhibitors interfere with retinal lamina formation both *in vivo* (Hamm *et al*., 1998) and *in vitro* (Layer *et al*., 1992). AChE could act either dependently, or, independently of its esterolytic activity. For instance, the release of ACh from navigating growth cones can attract or repulse certain neurites (Zheng *et al*., 1994); thereby, AChE would counteract any ACh signalling in its close vicinity. Alternatively, AChE can affect neurite growth nonenzymatically, possibly via a protein domain that is shared by all 'cholinesterase-like family' of cell adhesion molecules. It remains open whether an enzymatic and/or a nonenzymatic mechanism of AChE functions in the development of the mouse retina.

Conclusions

These findings document indispensable role(s) of AChE in both early retinal network formation and maintenance of retinal structure, not replaceable by the closely related butyrylcholinesterase. Ultimately this leads to photoreceptor degeneration. The AChE$^{-/-}$ mouse might serve as a novel model for retina formation and blinding diseases.

Acknowledgements

We thank D. Hicks, H.D. Hofmann, L. Peichl, A. Rothermel and E. Willbold for helpful discussions. We acknowledge the expert technical assistance by J. Huhn and M. Stotz-Reimers. This work was supported by the Deutsche Forschungsgemeinschaft (La 379/12–1), the German-Israeli-Foundation (G.I.F. 512/96), EU contract SENS-PESTI, QLK4-CT-2002–02264, and DAMD17-01-2-0036.

Abbreviations

AChE, acetylcholinesterase; BchE, butyrylcholinesterase; CB, calbindin; DAPI, 4′,6-diamidine-2-phenylindole-dihydrochloride; GCL, ganglion cell layer; INL, inner nuclear layer; IPL, inner plexiform layer; ONL, outer nuclear layer; OPL, outer plexiform layer; P, postnatal day; PBS, phosphate buffered saline, rho4D2, rod-specific antibody.

References

Aguirre, G.D., Yashar, B.M., John, S.K., Smith, J.E., Breuer, D.K., Hiriyanna, S., Swaroop, A. & Milam, A.H. (2002) Retinal histopathology of an XLRP carrier with a mutation in the RPGR exon ORF15. *Exp. Eye Res.*, **75**, 431–443.

Baimbridge, K.G., Celio, M.R. & Rogers, J.H. (1992) Calcium-binding proteins in the nervous system. *TINS*, **15**, 303–308.

Banin, E., Cideciyan, A.V., Aleman, T.S., Petters, R.M., Wong, F., Milam, A.H. & Jacobson, S.G. (1999) Retinal rod photoreceptor-specific gene mutation perturbs cone pathway development. *Neuron*, **23**, 549–557.

Behra, M., Cousin, X., Bertrand, C., Vonesch, J.L., Biellmann, D., Chatonnet, A. & Strahle, U. (2002) Acetylcholinesterase is required for neuronal and muscular development in the zebrafish embryo. *Nature Neurosci.*, **5**, 111–118.

Bourne, M.C., Campbell, D.A. & Tansley, K. (1938) Retinits pigmentosa in rats. *Trans. Ophthalmol. Soc. UK*, **58**, 234–245.

Broide, R.S., Grifman, M., Loewenstein, A., Grisaru, D., Timberg, R., Stone, J., Shani, M., Patrick, J.W. & Soreq, H. (1999) Manipulations of ACHE gene expression suggest non-catalytic involvement of acetylcholinesterase in the functioning of mammalian photoreceptors but not in retinal degeneration. *Brain Res. Mol. Brain Res.*, **71**, 137–148.

Buznikov, G.A., Lambert, H.W. & Lauder, J.M. (2001) Serotonin and serotonin-like substances as regulators of early embryogenesis and morphogenesis. *Cell Tissue Res.*, **305**, 177–186.

Casini, G., Rickman, D.W. & Brecha, N.C. (1995) AII amacrine cell population in the rabbit retina: identification by parvalbumin immunoreactivity. *J. Comp. Neurol.*, **1**, 132–142.

Connell, G., Bascom, R., Molday, L., Reid, D., McInnes, R.R. & Molday, R.S. (1991) Photoreceptor peripherin is the normal product of the gene responsible for retinal degeneration in the rds mouse. *Proc. Natl Acad Sci. USA*, **88**, 723–726.

Cuenca, N., Haverkamp, S. & Kolb, H. (2000) Choline acetyltransferase is found in terminals of horizontal cells that label with GABA, nitric oxide synthase and calcium binding proteins in the turtle retina. *Brain Res.*, **878**, 228–239.

Dmitrieva, N.A., Pow. D.V., Lindstrom, J.M. & Keyser, K.T. (2003) Identification of cholinoceptive glycinergic neurons in the mammalian retina. *J. Comp. Neurol.*, **456**, 167–175.

Dowling, J.E. & Sidman, R.L. (1962) Inherited retinal dystrophy in the rat. *J. Cell Biol.*, **14**, 73–109.

Duysen, E.G., Stribley, J.A., Fry, D.L., Hinrichs, S.H. & Lockridge, O. (2002) Rescue of the acetylcholinesterase knockout mouse by feeding a liquid diet; phenoytpe of the adult acetylcholinesterase deficient mouse. *Dev. Brain Res.*, **137**, 43–54.

Farber, D.B., Heckenlively, J.R., Sparkes, R.S. & Bateman, J.B. (1991) Molecular genetics of retinitis pigmentosa. *West J. Med.*, **155**, 388–399.

Fisher, S.K., Stone, J., Rex. T.S., Linberg, K.A. & Lewis, G.P. (2001) Experimental retinal detachment: a paradigm for understanding the effects of induced photoreceptor degeneration. *Prog. Brain Res.*, **131**, 679–698.

Grisaru, D., Sternfeld, M., Eldor, A., Glick, D. & Soreq, H. (1999) Structural roles of acetylcholinesterase variants in biology and pathology. *Eur. J. Biochem.*, **264**, 672–686.

Hamm, J.T., Wilson. B.W. & Hinton, D.E. (1998) Organophosphate-induced acetylcholinesterase inhibition and embryonic retinal cell necrosis *in vivo* in the teleost (*Oryzias latipes*). *Neurotoxicology*, **19**, 853–869.

Jeon, J., Kitamura, T., Yoo, B.W., Kang, S.O. & Ko, J. (2001) Synthesis and reactivity of an efficient 1,2-dehydrocarborane precursor, phenyl [o(trimethylsilyl)carboranyl]iodonium acetate. *Chem. Commun.*, **20**, 2110–2111.

Johnson, P.T., Raven, M.A. & Reese, B.E. (2001) Disruption of transient photoreceptor targeting within the inner plexiform layer following early ablation of cholinergic amacrine cells in the ferret. *Vis. Neurosci.*, **18**, 741–751.
Johnson, C.D. & Russell, R.L. (1975) A rapid, simple radiometric assay for cholinesterase, suitable for multiple determinations. *Anal. Biochem.*, **64**, 229–238.
Kablar, B. (2003) Determination of retinal cell fates is affected in the absence of extraocular striated muscles. *Dev. Dyn.*, **226**, 478–490.
Kater, S.B. & Lipton, S.A. (1995) Neurotransmitter regulation of neuronal outgrowth, plasticity and survival in the year 2001. *TINS*, **18**, 71–72.
Lauder, J.M. & Schambra, U.B. (1999) Morphogenetic roles of acetylcholine. *Environ. Health Perspect.*, **1**, 65–69.
LaVail, M.M. (1981) Photoreceptor characteristics in congenic strains of RCS rats. *Invest. Ophthalmol. Vis. Sci.*, **20**, 671–675.
LaVail, M.M. (2001) Legacy of the RCS rat: impact of a seminal study on retinal cell biology and retinal degenerative diseases. *Prog. Brain Res.*, **131**, 617–627.
Layer, P.G. (1990) Cholinesterases preceding major tracts in vertebrate neurogenesis. *Bioessays*, **12**, 415–420.
Layer, P.G., Berger, J. & Kinkl, N. (1997) Cholinesterases precede 'ON-OFF' channel dichotomy in the embryonic chick retina before onset of synaptogenesis. *Cell Tissue Res.*, **288**, 407–416.
Layer, P.G., Weikert, T. & Willbold, E. (1992) Chicken retinospheroids as developmental and pharmacological in vitro models: acetylcholinesterase is regulated by its own and by butyrylcholinesterase activity. *Cell Tissue Res.*, **268**, 409–418.
Layer, P.G. & Willbold, E. (1995) Novel functions of cholinesterases in development, physiology and disease. *Progr. Histochem. Cytochem.*, **29**, 1–94.
Li, B., Stribley, J.A., Ticu, A., Xie, W., Schopfer, L.M., Hammond, P., Brimijoin, S., Hinrichs, S.H. & Lockridge, O. (2000) Abundant tissue butyrylcholinesterase and its possible function in the acetylcholinesterase knockout mouse. *J. Neurochem.*, **75**, 1320–1331.
Li, L.X. & Turner, J.E. (1988) Inherited retinal dystrophy in the RCS rat: prevention of photoreceptor degeneration by pigment epithelial cell transplantation. *Exp. Eye Res.*, **47**, 911–917.
Lolley, R.N., Farber, D.B., Rayborn, M.E. & Hollyfield, J.G. (1977) Cyclic GMP accumulation causes degeneration of photoreceptor cells: simulation of an inherited disease. *Science*, **196**, 664–666.
Mesulam, M.M., Guillozet, A., Shaw, P., Levey, A., Duysen, E.G. & Lockridge, O. (2002) Acetylcholinesterase knockouts establish central cholinergic pathways and can use butyrylcholinesterase to hydrolyze acetylcholine. *Neuroscience*, **110**, 627–639.
Molday, R.S. (1988) Monoclonal antibodies to rhodopsin and other proteins of rod outer segments. [In Osborne, N.N. & Chader, G. (Eds)] *Prog. Retinal Res.*, **8**, 173–209.
Molday, R.S. (1998) Photoreceptor membrane proteins, phototransduction, and retinal degenerative diseases. The Friedenwald Lecture. *Invest. Ophthamol. Vis. Sci.*, **39**, 2491–2513.
Pasteels, B., Rogers, J., Blachier, F. & Pochet, R. (1990) Calbindin and calretinin localization in retina from different species. *Vis. Neurosci.*, **5**, 1–16.
Prada, F.A., Quesada, A., Dorado, M.E., Chmielewski, C. & Prada, C. (1988) Glutamine synthetase activity and spatial and temporal patterns of GS expression in the developing chick retina: relationship with synaptogenesis in the outer plexiform layer. *Glia*, **22**, 221–236.
Radic, Z. & Taylor, P. (2001) Interaction kinetics of reversible inhibitors and substrates with acetylcholinesterase and its fasciculin 2 complex. *J. Biol. Chem.*, **276**, 4622–4633.
Reiss, Y., Layer, P.G. & Kroger, S. (1997) Butyrylcholinesterase-positive cells of the developing chicken retina that are non-cholinergic and GABA-positive. *Brain Res. Dev. Brain Res.*, **100**, 62–72.
Scher, J., Wankiewicz, E., Brown, G.M. & Fujieda, H. (2003) AII amacrine cells express the MT(1) melatonin receptor in human and macaque retina. *Exp. Eye Res.*, **77**, 375–382.
Scholl, F.G. & Scheiffele, P. (2003) Making connections: cholinesterase-domain proteins in the CNS. *TINS*, **26**, 618–624.
Sernagor, E., Eglen, S.J. & Wong, R.O. (2001) Development of retinal ganglion cell structure and function. *Prog. Retin. Eye Res.*, **20**, 139–174.
Travis, G.H., Brennan, M.B., Danielson, P.E., Kozak, C.A. & Sutcliffe, J.G. (1989) Identification of a photoreceptor-specific mRNA encoded by the gene responsible for retinal degeneration slow (rds). *Nature*, **338**, 70–73.
Wässle, H., Grunert, U. & Röhrenbeck, J. (1993) Immunocytochemical staining of AII-amacrine cells in the rat retina with antibodies against parvalbumin. *J. Comp. Neurol.*, **4**, 407–420.
Willbold, E. & Layer, P.G. (1998) Muller glia cells and their possible roles during retina differentiation *in vivo* and *in vitro*. *Histol. Histopathol.*, **13**, 531–552.
Wong, W.T., Myhr, K.L., Miller, E.D. & Wong, R.O. (2000) Developmental changes in the neurotransmitter regulation of correlated spontaneous retinal activity. *J. Neurosci.*, **20**, 351–360.
Xie, W., Stribley, J.A., Chatonnet, A., Wilder, P.J., Rizzino, A., McComb, R.D., Taylor, P., Hinrichs, S.H. & Lockridge, O. (2000) Postnatal developmental delay and supersensitivity to organophosphate in gene-targeted mice lacking acetylcholinesterase. *J. Pharm. Exp.*, **293**, 896–902.
Yamada, E.S., Dmitrieva, N., Keyser, K.T., Lindstrom, J.M., Hersh, L.B. & Marshak, D.W. (2003) Synaptic connections of starburst amacrine cells and localization of acetylcholine receptors in primate retinas. *J. Comp. Neurol.*, **461**, 76–90.
Zheng, J.Q., Felder, M., Connor, J.A. & Poo, M.M. (1994) Turning of nerve growth cones induced by neurotransmitters. *Nature*, **368**, 140–144.
Zhou, Z.J. (1998) Direct participation of starburst amacrine cells in spontaneous rhythmic activities in the developing mammalian retina. *J. Neurosci.*, **18**, 4155–4165.
Zhou, Z.J. (2001) The function of the cholinergic system in the developing mammalian retina. *Prog. Brain Res.*, **131**, 599–613.